Article

Time–Temperature Superposition for Viscoelastic Properties of Regioregular Poly(3-hexylthiophene) Films

A. Robert Hillman, Igor Efimov, and Magdalena Skompska

J. Am. Chem. Soc., **2005**, 127 (11), 3817-3824• DOI: 10.1021/ja0437508 • Publication Date (Web): 01 March 2005

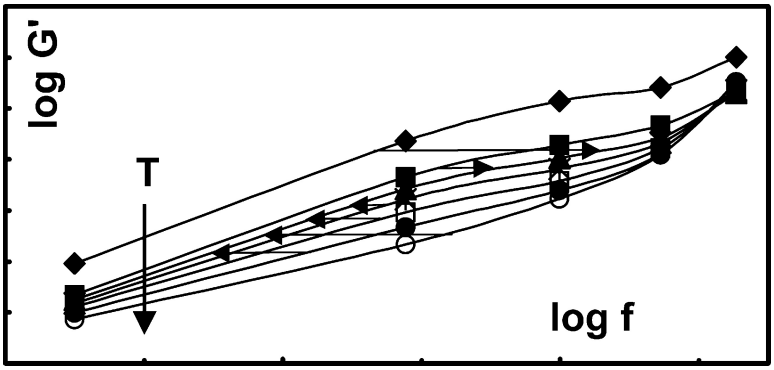

More About This Article

Additional resources and features associated with this article are available within the HTML version:

- Supporting Information
- Links to the 3 articles that cite this article, as of the time of this article download
- Access to high resolution figures
- Links to articles and content related to this article
- Copyright permission to reproduce figures and/or text from this article

View the Full Text HTML

J|A|C|S
ARTICLES
Published on Web 03/01/2005

Time−Temperature Superposition for Viscoelastic Properties of Regioregular Poly(3-hexylthiophene) Films

A. Robert Hillman,*,† Igor Efimov,† and Magdalena Skompska‡

Contribution from Department of Chemistry, University of Leicester, Leicester LE1 7RH, U.K., and Department of Chemistry, Warsaw University, 02 093 Warsaw, Poland

Received October 14, 2004; E-mail: arh7@le.ac.uk

Abstract: Shear moduli were determined for chemically polymerized and solvent cast regioregular poly(3-hexylthiophene) films, using thickness shear mode acoustic wave resonators. The results are strikingly different to those for electropolymerized regiorandom poly(3-hexylthiophene) films. The time scale of the measurement was varied directly by use of higher harmonics of the acoustic wave resonator and indirectly via temperature. The significant variations in shear modulus with effective time scale can be "normalized" onto a stress master relaxation curve by using the concept of time−temperature superposition; this is the first time this has been demonstrated for electroactive films. The shift factors required to effect this normalization do not follow the classical Williams−Landel−Ferry (WLF) equation developed for long-range backbone motions of bulk polymers. Instead, they follow an Arrhenius-like behavior, commonly used to describe secondary motions of polymer side-chains. The activation enthalpy associated with this is independent of applied potential, is the same as for *as cast* (undoped) films, and is similar to that for rotation about a carbon−carbon single bond. These all point to the hexyl side-chains as the origins of the observed phenomena, consistent with the "melting point" separating two temperature-dependent phases and with the different molecular packing arrangements that would necessarily apply to regioregular and regiorandom materials.

Introduction

Overview. In this paper we explore, for the first time, the extent to which the principle of time−temperature superposition can be applied to a thin electroactive polymer film. The goal is to combine data acquired under different conditions (of time scale and temperature) in such a manner as to place them on a common "time scale" axis and thereby explore the master relaxation curve; typically,[1,2] this extends over a wide range of time scales, such that the window provided by a single data set is inadequate to provide useful insight. Indeed, even the minority of studies of electroactive polymer film dynamics that are quantitative (in terms of shear modulus components) are generally restricted to a single value at fixed temperature and observational frequency. The unique fundamental feature of the present study is the manipulation of the normalized time scale of the system through three control parameters: applied potential, acoustic wave device frequency, and temperature. Respectively, these operate indirectly by influencing electrostatic stiffening and solvent plasticization, directly via observational time scale and directly through variation of polymer relaxation rate. Together, these three control parameters open an unusually wide window on the master relaxation curve. The practical significance of this is the extent to which it is appropriate to take a *macroscopic* concept from polymer science and apply it to materials used on *microscopic* scales relevant to nanoscience-based applications.

Motivation. The principle of time−temperature superposition is a powerful and well-established concept for rationalizing relaxation phenomena in *bulk* polymeric materials. Qualitatively, it expresses the notion (described below and elsewhere[1,2]) that polymer dynamics data acquired at different temperatures, and for which different relaxation rates apply, can be placed upon a single (master) relaxation curve by means of a "shift" factor, a_T. If the polymer dynamics are quantified in terms of the shear modulus, $G(T,t)$, acquired at two temperatures T_1 and T_2, for which different relaxation rates apply, then:

$$G(T_1,t) = G(T_2,t/a_T) \quad (1)$$

In terms of the angular frequency (ω) in a modulation experiment and the characteristic relaxation time (τ) of the system, which is a function of temperature, this means that one can find a corresponding frequency of mechanical excitation at which **G** measured at two different temperatures will be the same. In the most common case, the mechanical properties depend on the product $\omega\tau$. If one knows the manner in which relaxation rate varies with temperature, the shift factor can be predicted. Conversely, if the shift factor required to place the responses on a single curve is determined, then one has access to the energetics of the system and thereby insight into the underlying physicochemical processes. Classically, the procedure has been

† University of Leicester.
‡ Warsaw University.

(1) Ferry, J. D. *Viscoelastic Properties of Polymers*, 2nd ed.; Wiley: New York, 1970.
(2) Aklonis, J. J.; MacKnight, W. J. *Introduction to Polymer Viscoelasticity*, 2nd ed.; Wiley: New York, 1983.

used[1] to rationalize creep behavior of bulk polymers at changing temperatures. The postulate is that mechanical properties depend on the product $\omega\tau(T)$ of angular frequency (ω) and characteristic relaxation time (τ), which is a function of temperature (T). The consequence is that, if the temperature is changed, one can find a corresponding frequency of mechanical excitation at which mechanical properties will be the same. For a given frequency, measurements at different temperatures represent different parts of the relaxation spectrum.

The concept has been widely considered for *bulk* polymer components, by determining shear modulus (or compliance) data, commonly at low frequencies associated with classical electromechanical devices. We[3−6] and others[7,8] have recently developed the capability to determine shear moduli for thin polymer films loaded onto high frequency (MHz) acoustic wave devices. The dimensions (10 nm to 10 μm) of such films are typical of practical applications in electrochemistry specifically and nanoscience generally: examples include sensors,[9] energy conversion[10]/storage,[11] electrochromic devices,[12] molecular electronic devices,[13] micromechanical actuators,[14] and electrocatalysis.[15] Quite generally, for polymeric materials in the form of a *thin film* with characteristic dimensions commensurate with polymer chain length, the issue arises as to whether *macroscopic* concepts can be applied on the *micro-* and *nanoscale*. The specific case of time−temperature superposition is particularly relevant to electrochemically based devices since a common anecdotal observation is that polymer dynamics are the slowest of the various elementary steps involved in film redox switching. Thus, they may control device response rate, sensitivity, or long-term reproducibility—all of which are critical to practical viability.

We therefore set out to explore whether the normalization process associated with the "shift factor" approach could be applied to materials of interest to the (electro)chemical applications listed above. Previous experience of electropolymerized conducting polymers[16] indicated that their structures and compositions may be less easy to control from sample to sample; variable chain length, uncontrolled cross-linking, and regiorandom structures (with regard to disposition of the alkyl side group) are probably the underlying structural issues. In contrast, chemically polymerized materials offer opportunities to control regioregularity and to separate materials of different composition, chain length, and structure. Accordingly, we have found that cast films of *regioregular* poly(3-hexylthiophene) (P3HT)—which we study here—are more reproducible[6] and have more tractable behavior than their electropolymerized *regiorandom* counterparts.[3,4]

Target System. P3HT is thermochromic semicrystalline polymer representative of the hugely studied thiophene-based family of conducting polymers.[17] The degree of crystallinity is sensitive to the degree of regioregularity:[18] for *regioregular* P3HT (about 97% HT coupling), the material studied here, the crystallinity is about 25−30%.[19] For a given material, the relative contributions of amorphous and crystalline structures[20] depend on crystallization temperature and thermal history of the sample. The coexistence of polycrystalline and amorphous phases in P3HT films has been confirmed by STM images;[21] the consequences on electronic structure are seen in the UV−visible spectrum[22] and the electrochemical response, which shows several oxidation peaks according to regioregularity.[23] During doping, the first (less positive) voltammetric peak, corresponding to oxidation of more ordered, polycrystalline phase, is concomitant with bleaching of a long wavelength shoulder in the UV−visible absorption band ($\pi \rightarrow \pi^*$ transition), whereas the more anodic peak corresponds to oxidation of an amorphous polymer phase associated with the main absorption band maximum. This pattern was the most pronounced for polymer with the highest regioregular head-to-tail (HT−HT) content (97%). This conclusion was supported by increase of doping level and conductivity of P3HT films of higher HT−HT content.[24] It is reasonable to propose that chain structure, notably, regioregularity, controls both electronic properties per se and polymer dynamics. This is a specific example of the general observation that quantitative studies of polymer dynamics are rare, despite wide recognition that they strongly influence rates of mobile species (ion, solvent, and reactant) permeation and thus of redox switching.

Strategy. The most common energy input to the system in the electrochemical context is applied potential; temperature is a much underexploited variable in this context. A novel feature of the present study is the use of both potential and temperature as variables in the determination of film dynamics. In doing so, we recognize two temperature effects: the variation in the proportions of the two phases and their individual relaxation rates. The former is specific to the system studied, and the latter has generic relevance. The combination of electrochemical and acoustic wave studies provides a unique perspective on these interlocked phenomena.

(3) Brown, M. J.; Hillman, A. R.; Martin, S. J.; Cernosek, R. W.; Bandey, H. L. *J. Mater. Chem.* **2000**, *10*, 115−126.
(4) Skompska, M.; Jackson, A.; Hillman, A. R. *Phys. Chem. Chem. Phys.* **2000**, *2*, 4748−4757.
(5) Hillman, A. R.; Jackson, A.; Martin, S. J. *Anal. Chem.* **2001**, *73*, 540−549.
(6) Hillman, A. R.; Efimov, I.; Skompska, M. *Faraday Discuss.* **2002**, *121*, 423−439.
(7) Etchenique, R. A.; Calvo, E. J. *Electrochem. Comm.* **1999**, *1*, 167−170.
(8) (a) Calvo, E. J.; Forzani, E.; Otero, M. *J. Electroanal. Chem.* **2002**, *538*, 231−241. (b) Calvo, E. J.; Forzani, E. S.; Otero, M. *Anal. Chem.* **2002**, *74*, 3281−3289. (c) Vago, M.; Campodall'Orto, V.; Rezzano, I.; Forzani, E. S.; Calvo, E. J. *J. Electroanal. Chem.* **2004**, *566*, 177−185.
(9) (a) Welzel, H. P.; Koβmehl, G.; Schneider J.; Plieth, W. *Macromolecules* **1995**, *28*, 5575−5580. (b) Piro B.; Dang L. A.; Pham M. C.; Fabiano S.; Tran-Minh C. *J. Electroanal. Chem.* **2001**, *512*, 101−109.
(10) (a) Ohmori, Y.; Uchida, M.; Muro, K.; Yoshino, K. *Sol. State Commun.* **1991**, *80* 605−608. (b) Pei, Q.; Yu, G.; Zhang, C.; Yang, Y.; Heeger, A. J. *Science* **1995**, *269*, 1086−1088.
(11) Nishino, K.; Fujimoto, M.; Yoshinaga, N.; Furukawa, N.; Ando, O.; Ono, H.; Suzuki, T. J. *Power Sources* **1991**, *34*, 153−160.
(12) Gustafsson, J. C.; Liedberg, B.; Inganäs, O. *Solid State Ionics* **1994**, *69*, 145−152.
(13) (a) Scrosati, B. In *Application of Electroactive Polymers*; Chapman and Hall: New York, 1993. (b) Skotheim, T. A.; Elsenbaumer, R. L.; Reynolds, J. R. In *Handbook of Conducting Polymers*; Marcel Dekker: New York, 1998.
(14) Jager, E. W. H.; Inganäs, O.; Lundström, I. *Science* **2000**, *288*, 2335−2338.
(15) Malinauskas, A. *Synth. Met.* **1999**, *107*, 75−83.
(16) Roncali, J. *Chem. Rev.* **1992**, *92*, 711−738.
(17) (a) McCullough, R. D. *Adv. Mater.* **1998**, *10*, 93−116. (b) Schopf, G.; Koβmehl, G. In *Polythiophenes-Electrically Conductive Polymers, Advances in Polymer Science*; Springer: Berlin, 1997; Vol. 129, pp 3−145.
(18) Yang, C.; Orfino, F. P.; Holdcroft S. *Macromolecules* **1996**, *29*, 6510−6517.
(19) Łużny, W.; Trznadel, M.; Proń, A. *Synth. Met.* **1996**, *81*, 71−74.
(20) Zhao, Y.; Yuan, G.; Roche, P.; Leclerc, M. *Polymer* **1995**, *36*, 2211−2214.
(21) Grévin, B.; Rannou, P.; Payerne, R.; Pron, A.; Travers, J.-P. *Adv. Mater.* **2003**, *15*, 881−884.
(22) (a) Winokur, M. J.; Spiegel, D.; Kim, Y.; Hotta, S.; Heeger, A. J. *J. Synth. Met.* **1989**, *28*, C419−C426; Park, K. C.; Levon, K. *Macromolecules* **1997**, *30*, 3175−3183. (c) McCullough, R. D.; Lowe, R. D.; Jayaraman, M.; Anderson, D. L. *J. Org. Chem.* **1993**, *58*, 904−912.
(23) Skompska, M.; Szkurlat, A. *Electrochim. Acta* **2001**, *46*, 4007−4015.
(24) Jiang, X.; Harima, Y.; Yamashita, K.; Tada, Y.; Ohshita, J.; Kunai, A. *Chem. Phys. Lett.* **2002**, *364*, 616−620.

On the basis of the notion that polymer phases with different crystallinity have different redox potentials, the proportions of the different phases can be determined by coulometric assay of the respective peaks in the voltammetric response. Variations in the coulometric assay with temperature then provide the variation of the amorphous/crystalline equilibrium with temperature. At any given potential, temperature variations predominantly reflect the changing relaxation characteristics of the material; these are accessed via film shear modulus, $\mathbf{G} = G' + jG''$, where G' is the storage modulus and G'' is the loss modulus. Quite generally, one would expect **G** to respond to the stiffness of individual chains, to the electrostatic interactions between them, and to the presence of small molecules (solvent) separating them. All of these may be manipulated by electrochemical control of polymer redox state, the first two directly (in terms of charge density and delocalization) and the latter indirectly (as a consequence of the constraint of constant solvent activity).[25] The expectation is that all these effects will change the mechanical properties of the polymer: the electrostatic effects should stiffen the film and entry of solvent should plasticize it.

The strategy then is to use the piezoelectric characteristics of the quartz resonator to measure the mechanical impedance of the film; this in turn yields **G** and thus G' and G''. Limited direct exploration of the time scale—an order of magnitude—is possible via measurements at the fundamental frequency and at higher harmonics. Measurements as a function of temperature provide the test of time−temperature superposition, which has not been addressed for electroactive thin films.

Experimental Section

Films of P3HT (97% HT−HT; Aldrich) were cast from chloroform solution onto thin film Au electrodes, as described elsewhere.[6] Polymer surface coverages (Γ/mol cm^{-2}) are derived from application of Faraday's law to integrated slow scan voltammetric responses and are expressed in terms of moles of monomer units, based on a maximum doping level of 0.3.[6] The Au electrode (piezoelectric and electrochemically active areas 0.23 and 0.25 cm^2, respectively) was one of the exciting electrodes on a 10-MHz AT cut quartz crystal resonator (ICM, Oklahoma City, OK). Polished crystals were used to minimize effects associated with surface roughness.[4,5] The coated electrode formed the working electrode in a three-electrode cell, with a platinum foil counter electrode and silver wire reference electrode. The potential of this reference electrode was −0.26 V vs Ag^+/Ag^0 (0.1 M, CH_3CN) (calibrated using the ferrocene/ferricenium couple); to facilitate literature comparisons, all potentials are quoted with respect to the Ag^+/Ag^0 reference electrode. The solution for all electrochemical measurements was 0.1 M $LiClO_4$/acetonitrile. Reagents and other general procedures were as described elsewhere.[6] Crystal impedance spectra were recorded using a Hewlett-Packard HP8751A network analyzer, connected to a HP87512A transmission/reflection unit via 50 Ω coaxial cable. The electrochemical cell was immersed in a thermostatic bath, allowing measurements to be conducted over the temperature range 0−70 °C. For the study reported here, it was necessary to characterize the solution parameters ρ_l and η_l (ρ_l is the density and η_l is the dynamic viscosity of the solution) as functions of temperature; numerical data were consistent with standard literature values.

Interpretation of experimental crystal admittance spectra to obtain the four parameters that characterize the film (thickness, h_f, density, ρ_f, storage modulus, G', and loss modulus, G'') was based on a method described elsewhere.[5] In overview, cyclic voltammetry and admittance spectra were recorded first for the acoustically thin film. Mass changes in this case can (by definition) be calculated directly from the resonant frequency shift, according to the Sauerbrey equation. Application of Faraday's law to the charge under the cyclic voltammogram gives the number of moles of monomer deposited per unit area;[6] we used the conventional value of 0.3 for the number of electrons per thiophene ring transferred during the (un)doping process. From these two sets of data, film density and thickness (at given total reduction charge) were calculated according to the procedure described elsewhere.[6] For acoustically thick films, used in experiments shown here, the density was assumed to be the same as for a thin film; film thickness was scaled according to total film redox charge.

The network analyzer measures admittance curves, which give the electrical impedance linearly related to the acoustic impedance, Z, of the compound resonator comprising quartz, polymer film, and semi-infinite solution. The values of G' and G'' of the polymer were calculated numerically (by using the Maple program) as complex roots of eq 2, which relates the experimentally measured mechanical impedance to the impedances of its separate elements:[6]

$$Z = j\omega\rho_s + Z_P\left(\frac{Z_L\cosh(\gamma h_f) + Z_P\sinh(\gamma h_f)}{Z_P\cosh(\gamma h_f) + Z_L\sinh(\gamma h_f)}\right) \qquad (2)$$

In eq 2, Z_P is the mechanical impedance of the film, defined as $Z_P = (G\rho_f)^{1/2}$, Z_L is the mechanical impedance of the electrolyte solution (a semi-infinite Newtonian fluid) at the film, $Z_L = (\omega\rho_L\eta_L/2)^{1/2}(1+j)$, and ρ_L and η_L are, respectively, the solution density and solution viscosity. The first term in eq 2 accounts for surface roughness of material, which can be interpreted as "rigidly coupled" mass with surface density ρ_s (g cm^{-2}); although the procedure accounts for this term, its contribution is minimized by use of polished crystals.[5,6]

Results

We identify two distinct temperature effects: on the position of equilibrium between two polymer structures and on polymer dynamics. The former, which we discuss first, is specific to this chemical system and is manifested primarily through the electrochemical response. We then go on to discuss polymer dynamics per se, which are manifested through the acoustic resonator response; this generic issue is the primary thrust of the work. In this latter instance, the effects observed are demonstrably a function of both temperature and time scale (frequency, via resonator harmonic). Thus, one is not dealing with a simple crystallization process, which would be independent of time scale (frequency).

Electrochemical and Resonant Frequency Responses to Temperature. Figure 1 shows slow scan rate (10 mV s^{-1}) cyclic voltammetric responses for a representative regioregular P3HT film in 0.1 M $LiClO_4$/acetonitrile as a function of temperature. The striking feature is the decrease in peak current (and charge) for the first oxidation peak and its shift toward less positive potentials with increasing temperature. In this slow scan rate regime, the peak current is linear with potential scan rate (υ) and the total switching charge passed is independent of υ; thus, we have full redox conversion of the film on the time scale of a complete redox cycle. The total charge, Q_{max}, (including both peaks and integrated over the range $-0.1 < E/V < 0.93$) was 4.50 mC cm^{-2} for oxidation and 4.17 mC cm^{-2} for reduction. We attribute the slight difference to background currents at positive potentials; on this basis, charges for film reduction were used for the purposes of coulometric assay. The key result, necessary for the interpretation below, is that these values showed no trend with temperature.

(25) Bruckenstein, S.; Hillman, A. R. *J. Phys. Chem.* **1988**, *92*, 4837−4839.

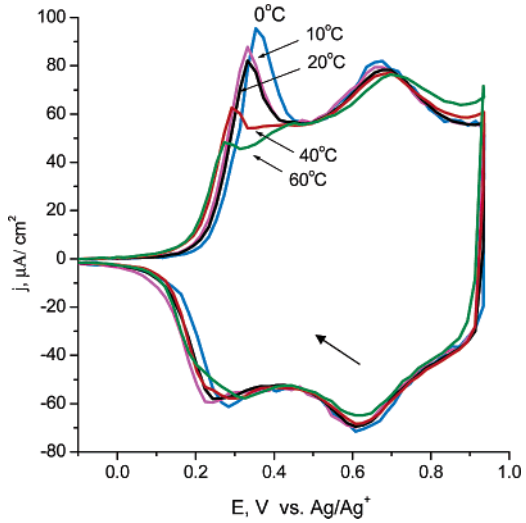

Figure 1. Cyclic voltammetric responses for a regioregular P3HT film (cast on Au and exposed to 0.1 M $LiClO_4$/acetonitrile) at various temperatures (as indicated). Polymer surface concentration, $\Gamma = 144$ nmol cm^{-2}; in the absence of solvent, this would correspond to an oxidized film thickness, $h_f = 0.28$ μm. Scan rate, $\nu = 10$ mV s^{-1}.

The change of thickness, h_f, of regioregular PH3T films as a function of potential was measured from resonant frequency data for acoustically thin films.[6] Film thickness values (required to determine shear moduli) for acoustically thick films were then determined by simple proportionality to redox switching charge for each individual film; the same proven strategy[6] was used here. Commencing from a fully reduced film, h_f-E responses show significant increases at 0.6−0.7 V, similar to AFM data for P3HT in propylene carbonate 0.1 M $LiClO_4$.[26] In principle, although Q_{max} was constant over the temperature range explored, h_f is a function of temperature. We assume that this deviation is small compared to the other variations in film properties.

The charge, Q_1, under the first peak in the cyclic voltammograms shown in Figure 1 represents the most readily oxidized phase (previously identified as crystalline[6]). The remaining charge, (Q_{max}-Q_1), represents the least readily oxidized phase (previously identified as amorphous[6]). Thus, the position of equilibrium between these two can be expressed in terms of the equilibrium constant, K, related to the charge and the underlying thermodynamic parameters by

$$K = \frac{Q_{am}}{Q_{cryst}} = \frac{Q_{max} - Q_1}{Q_1} \quad (3)$$

$$\ln K = -\frac{\Delta G^0}{RT} = -\frac{\Delta H^0}{R}\frac{1}{T} + \frac{\Delta S^0}{R} \quad (4)$$

Variation with temperature of the ratio of these two charges, representing the equilibrium constant for the interconversion of the phases, is shown in Figure 2. From the slope and intercept, respectively, of Figure 2 we obtain $\Delta H^0 = 9.7$ kJ mol^{-1} and $\Delta S^0 = 46$ J mol^{-1} K^{-1} for the conversion of the crystalline phase to the amorphous phase. These values are qualitatively consistent with the anticipated endothermic and disordering nature of "melting" of a crystalline phase to an amorphous one.

(26) Skompska, M.; Szkurlat, A.; Kowal, A.; Szklarczyk, M. *Langmuir* **2003**, *19*, 2318−2324.

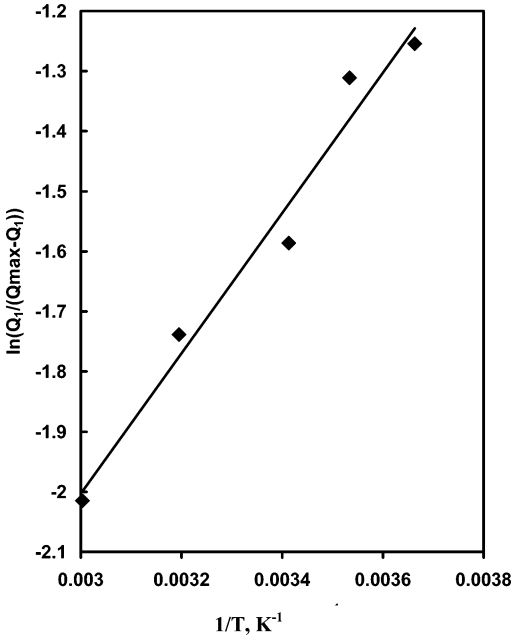

Figure 2. Variation of charge distribution under voltammetric peaks (see Figure 1) with temperature.

We note that this simple treatment, which appears to adequately describe the data, assumes that the redox centers are noninteracting and embedded in one of the two (crystalline or amorphous) phases; strictly, it would also apply if there were identical interactions between redox sites of either type.

The resonant frequency changes, Δf, as a function of potential show hysteresis (according to the potential scan direction) but relatively little variation with temperature. Crystal admittance responses (see below) unquestionably show the films to be viscoelastic, most simplistically through the nonzero resonant resistance, which precludes quantitative interpretation of the resonant frequency in terms of the Sauerbrey equation.[27] Nonetheless, it is still useful to consider the frequency changes as a function of charge injected into the film since they give a qualitative indication of mass changes. Furthermore, regardless of interpretation, such plots indicate whether film solvation and mechanical properties are (or are not) equilibrated with redox state. Representative data are shown in Figure 3. These and analogous data show that, across the temperature and charge level ranges explored, film solvation is approximately equilibrated with charge state. This allows the considerable practical simplification that, at the level of precision of the experiment, the thickness variation with charge state is the same at all temperatures. The relatively small potential dependence of resonant resistance suggests that, although not used quantitatively, the Sauerbrey equation provides a rough guide to film mass changes. At this level of approximation, the slopes of the plots in Figure 3 indicate a mass change of ca. 300 g $equiv^{-1}$, which represents entry of ca. five molecules of solvent for every counterion.

Viscoelastic Responses to Temperature. Now that the distribution of phases with respect to temperature is determined, we proceed to determine their viscoelastic properties. These are extracted from the crystal admittance spectra and expressed through shear modulus storage and loss components, G' and

(27) Sauerbrey, G. *Z. Phys.* **1959**, *155*, 206−222.

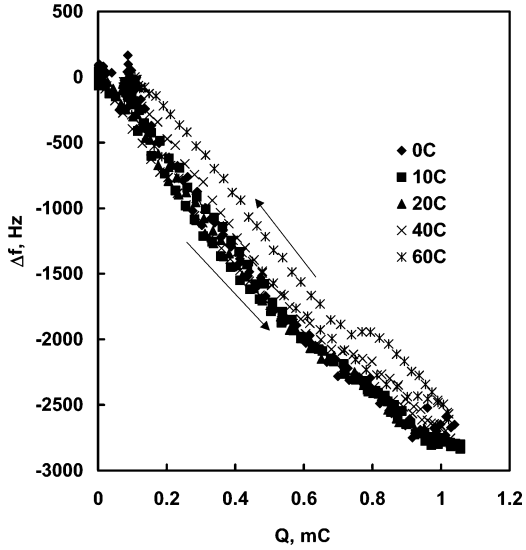

Figure 3. Frequency change as a function of injected charge (defined as $Q = 0$ at $E = -0.1$ V) during experiments of Figure 1. Temperatures as annotated. Arrows indicate scan direction.

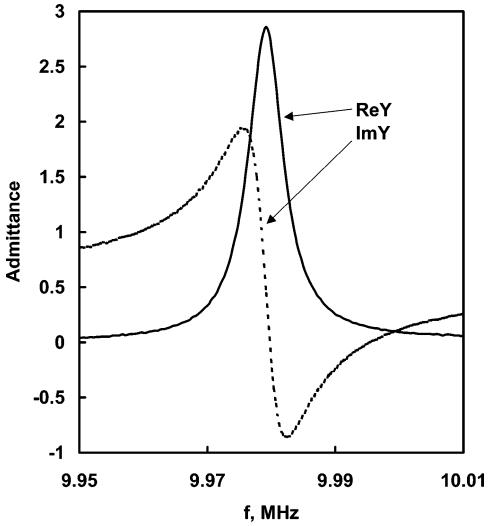

Figure 4. Representative admittance spectra for an *as cast* P3HT film exposed to 0.1 M $LiClO_4$/acetonitrile at $T = 20$ °C. Film as Figure 1 but prior to the experiment of Figure 1.

G''. We initially consider the properties of *as cast* films at open circuit; although not controlled directly, such films are nominally uncharged (undoped). We then go on to follow the variation of film properties with applied potential (and thus charge state). In the case of films returned to the uncharged (undoped) state, this will enable the influence of redox cycling to be deduced.

The admittance response for a representative *as cast* P3HT film ($\Gamma = 144$ nm cm^{-2}) exposed to $LiClO_4$/acetonitrile is shown in Figure 4. The data are clearly of high quality (high *S*/*N*) and reflect the significant losses associated with polymer properties (the admittance associated with a bare Au electrode in the electrolyte is ca. 6−7 mS). Storage (G') and loss (G'') moduli resulting from this and analogous spectra for varying conditions are shown in Figure 5, panels a and b, respectively. Our primary interest is in G' (the film stiffness); henceforth, we focus our attention on this component of the shear modulus. Qualitatively, at any given measurement frequency (time scale) one can see a progressive decrease in G' with increase in temperature.

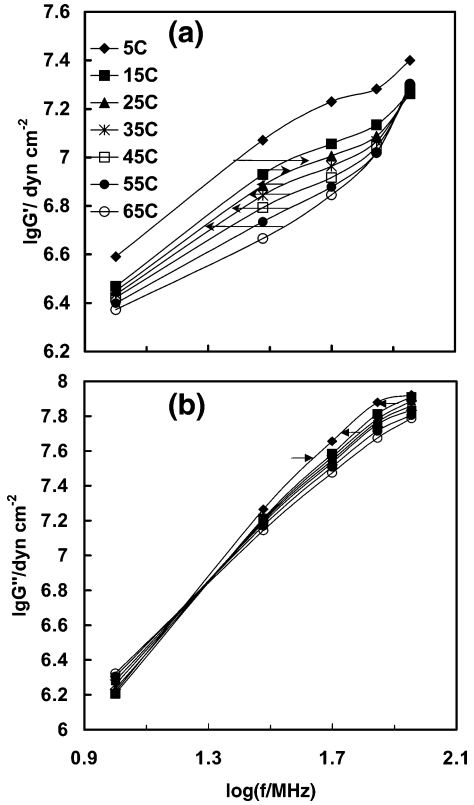

Figure 5. (a) Storage modulus, G' and (b) loss modulus, G'', as functions of frequency for a P3HT film (that of Figure 4) *as cast*, then exposed to 0.1 M $LiClO_4$/acetonitrile at open circuit. Temperature as annotated. Lowest frequency corresponds to fundamental resonance (10 MHz); other frequencies correspond to higher harmonics. Arrows indicate direction of "shift", by log $a(T)$, to construct master curve reduced to $T = 25$ °C.

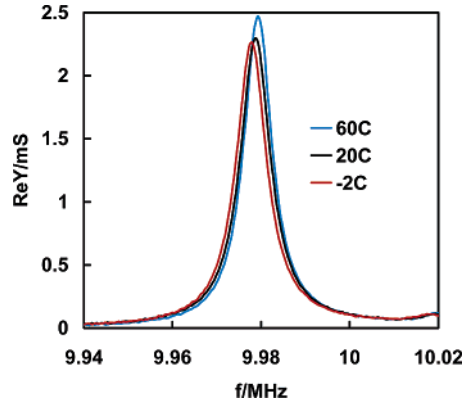

Figure 6. Representative admittance spectra for the P3HT film of Figure 1 at $E = 0.80$ V. Temperatures as indicated.

Following redox cycling (as shown in Figure 1), admittance spectra were acquired for the film held at fixed potentials; for purposes of illustration, we selected 0.0, 0.50, and 0.80 V, corresponding to fully reduced (undoped), partially oxidized, and fully oxidized (doped) states, respectively. Figure 6 shows representative admittance spectra for a film held at a potential of 0.80 V at three different temperatures. In viewing the changes seen in Figure 6 it should be borne in mind that, once the "background" changes associated with changing *solution* properties have been removed, the underlying *film* contributions—the object of the study—to this overall response in fact change rather more significantly than is obvious from the figure. Using

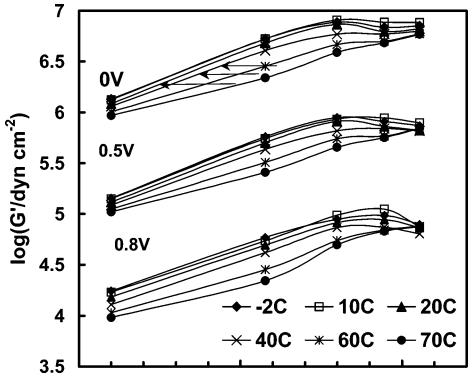

Figure 7. Storage modulus, G', as a function of frequency for a P3HT film (as Figure 1) exposed to 0.1 M $LiClO_4$/acetonitrile and maintained under potential control. Potential and temperature as annotated. Lowest frequency corresponds to fundamental resonance (10 MHz); other frequencies correspond to higher harmonics. Arrows indicate direction of "shift", by log $a(T)$, to construct master curve reduced to $T = 25$ °C.

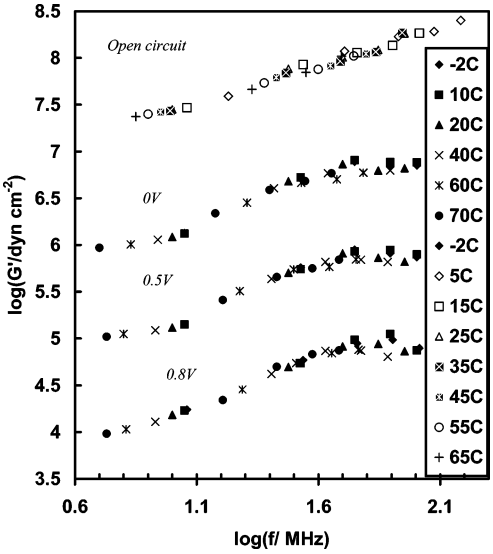

Figure 8. G' values as functions of f and T from Figure 5, and of f, T, and E from Figure 7, reduced to a common temperature ($T = 25$ °C), according to the "shift" procedure described in the text and indicated by the arrows of Figures 5 and 7. Potential and temperature as annotated.

the methodology described above, the data of Figure 6 yielded the shear storage modulus (G') values shown in Figure 7.

In all cases, the responses are characteristic of a viscoelastic material with T_g far below the temperature range studied and a loss tangent, G''/G', close to unity. This is consistent with the relatively low shear moduli observed, $\mathbf{G} \sim 10^7-10^8$ dyn cm^{-2}. At any given temperature, we are able to span approximately 1 order of magnitude in time scale (from the fundamental to ninth harmonic), which is clearly much less than the range of time scales associated with the transition from the rubbery to the glassy regime typical of bulk materials.[1] A surprising observation is that, despite the obvious compositional and structural changes, applied potential (and thus charge state) does not greatly change the viscoelastic properties. Qualitatively, we deduce that the opposing stiffening effects of the electrostatic forces and plasticizing effect of increased solvation with increasing potential (charge) broadly compensate each other. Comparison of the G' data in Figures 5 and 7, for the *as cast* and cycled films respectively, indicates that redox cycling and returning to the same state does not appreciably change the film viscoelastic properties. The key deduction from Figures 4−7 is that the influence of temperature is significant: explaining this is the key goal of the discussion that now follows.

Time−Temperature Equivalence. According to the principle of time−temperature equivalence,[1] it should be possible to superimpose the $G' - \log f$ curves in Figures 5 and 7 by adding a temperature-dependent factor log $a(T)$ to the abscissa (log f) scale. This so-called "shift factor" should be the same for all frequencies for a curve measured at a given temperature. To test this, one needs to select a reference point for the temperature scale (we chose $T = 25$ °C). The concept is illustrated by arrows indicating the directions of shift for the *as cast* film data in Figure 5a. It is implemented by optimizing the overlay of each individual temperature data set.

The results of applying this procedure to the G' values of Figures 5 and 7, respectively, for the *as cast* (open circuit) and potential controlled films are shown in Figure 8. It is a significant accomplishment that the dispersion of properties spanning a temperature range of 70 °C can be removed by application of time−temperature equivalence. Having demonstrated that the concept of time−temperature equivalence applies at a qualitative level for this material, we now seek to understand the underlying physical significance of the shift factors.

One description is the Williams−Landel−Ferry (WLF) model,[1,2] which considers long-range motions of the polymer chain above the glass transition temperature. The WLF model predicts that

$$\log a(T) = \frac{-C_1(T - T_g)}{C_2 + T - T_g} \tag{5}$$

where T_g is the glass transition temperature and C_1 and C_2 are constants. Since these long-range motions tend not to be especially sensitive to the detailed structural characteristics of the polymer, the constants have "universal" values, $C_1 = 17.44$ and $C_2 = 51.6$. Although this model has enjoyed considerable success for bulk polymers, we were not able to fit our data using eq 5.

In the case of P3HT, one must consider not only long-range backbone motions but also secondary motions in the side-chains. Such motions are clearly rather more specific to the material in question and less likely to be described by the WLF equation. It has been found (for bulk materials)[2] in such cases that the concept of time−temperature superposition applies but that the WLF equation does not apply. Instead, the shift factors have an Arrhenius-type dependence on temperature. One can calculate the associated activation enthalpy, ΔH_a, from the experimentally determined log $a(T)$ data according to[2]

$$\Delta H_a = 2.303R\frac{\partial \log a(T)}{\partial(1/T)} \tag{6}$$

The shift factors from the master curves for G' (Figure 8) are plotted according to eq 6 in Figure 9. The slopes for the four data sets (open circuit: 513 K^{-1}; 0 V: 513 K^{-1}; 0.5 V: 504 K^{-1}; 0.8 V: 497 K^{-1}) are identical, within the precision of the experiment, and yield $\Delta H_a = 9.7$ kJ mol^{-1}. This value for the relaxation barrier is comparable with the activation energy of rotation around C−C bonds, ca. 12.5 kJ mol^{-1}. Analogous

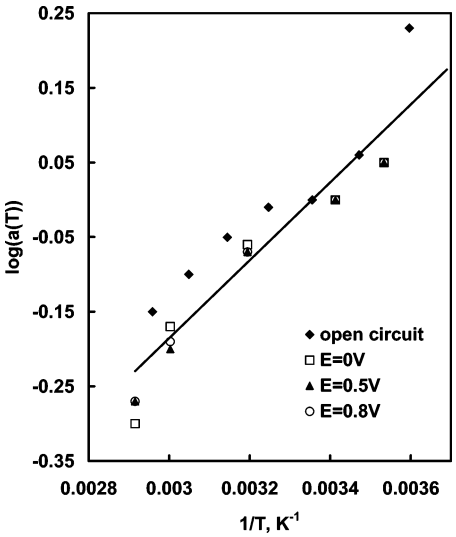

Figure 9. Variation of shift factors with temperature, plotted according to the Arrhenius-like dependence of eq 6. Data are those required to transform Figures 5 and 7 to Figure 8. Symbols as Figure 8.

treatment for the G'' shift factors produces a somewhat smaller value for the barrier energy; of course, the barrier is the same in both cases, but separate consideration of the two responses gives an idea of consistency. As an aside, we note that these estimates are somewhat smaller than, but on the same order of magnitude as, the high-temperature limit for ΔH_a in the WLF theory, $\Delta H_a(T \gg T_g) = 2.303RC_1C_2$, which has the numerical value of 14.4 kJ mol^{-1}.

All the above point to motions of the hexyl side groups as the origins of the observed dynamics. We note three additional factors that support this hypothesis. First, the relative rigidity of individual aromatic rings and the geometric constraint of coplanarity of adjacent rings for the extensive charge delocalization characteristic of conducting polymers suggest that the polymer backbone will be less flexible than the linear aliphatic side-chains. Thus, moderate temperatures are more likely to facilitate side-chain motion. Second, rotation of the conjugated aromatic rings would be associated with high and potential-(doping level-) dependent activation energies; we do not find this. A third, circumstantial piece of evidence is that the characteristic temperature for the crystalline/amorphous transition of alkyl side-chains, $\Delta H^0/\Delta S^0 = -62$ °C, is not too different from the melting point of hexane (−95 °C [28]); since adding a heavy atom (iodine) to the end of the C_6 chain raises the melting point of hexane by 20 °C, the observed "melting" point is a reasonable consequence of attachment to the polymer backbone. This dominance of the polymer dynamics by side-chain motion also rationalizes the fact that the behaviors of *regiorandom* (electropolymerized) and *regioregular* (chemically polymerized, according to selective linkages) materials—for which the only difference is the spatial disposition of side-chains—are very different.

In considering the value and assignment of the melting temperature, it is instructive to compare the present data with those for some related systems. DSC studies of regioregular poly(3-dodecylthiophene) showed melting temperatures of 59 and 114 °C, which were attributed to the side-chains and spine, respectively.[29] Another study of poly(3-dodecylthiophene) films found a T_g value of −16 °C, and a lower transition region covering the range 30−75 °C, which was assigned to side-chain melting.[30] Attachment of similar side-chains to a different (nonconducting) spine was found to have similar effects, in that poly(di-*n*-alkylsilane) films with C_6, C_7, and C_8 side-chains all showed melting temperatures in the range 40−50 °C, which were attributed to melting of these side-chains.[31] In the specific case of the C_6 side-chains, supercooling effects were found to result in crystallization temperature lowering by up to 12 °C. The same authors also noted that acrylate analogues may have amorphous main chains, even if side-chains show considerable tacticity.

The qualitative consensus of the above work is that side-chain melting for moderate length alkyl side-chains occurs before that of the main chain; this is consistent with our findings. The quantitative difference is that the melting points attributed to the side-chains in these studies are rather higher than found in our work: we need to address this discrepancy, particularly for the (apparently) similar alkylthiophene materials. Comparison of the techniques reveals the answer: the cited works relate to "dry" (solvent-free) films in a gaseous atmosphere, whereas our studies involved films exposed to a liquid phase. The consequence of exposure to liquid is a highly solvated film (here, on the order of 50 vol %).[6] This solvent plasticizes the film and significantly lowers the melting temperature. Although we have indicated previously[4,6] the importance of the solvent on film properties, this dramatically underscores the point.

Conclusions

We have explored, for the first time, the extent to which the principle of time−temperature superposition can be applied to a thin electroactive polymer film. An unusually wide window can be opened on the master relaxation curve by manipulating the normalized time scale of the system through three control parameters: applied potential, mechanical excitation frequency, and temperature. The combination of electrochemical and thermal energy inputs in the context of an acoustic wave device is a powerful one from a mechanistic perspective.

Spin cast *regioregular* P3HT films shows interconversion of two structurally distinct forms, nominally referred to as crystalline and amorphous. These two forms can be interconverted by variation of temperature.

Films in the *as cast* state and following electrochemical cycling show similar viscoelastic properties, parameterized via shear moduli. Surprisingly, variation of electrochemical potential (charge state) across a wide range of doping levels has little effect on shear moduli; we conclude that electrostatic stiffening associated with increased intra- and interchain interactions during doping is compensated by solvent plasticization.

Acoustic wave measurements at the resonator fundamental frequency and higher harmonics shows significant variation of shear moduli: decreasing time scale results in stiffening. Analogously, decreasing temperature results in stiffening at fixed frequency. The storage moduli can be placed on a master curve using the time−temperature superposition principle, originally

(28) *CRC Handbook of Chemistry and Physics*, 56th ed.; Weast, R. C., Ed.; CRC Press: Cleveland, 1975; p C-328.

(29) Liu, S. L.; Cheung, T. S. *Polymer* **2000**, *41*, 2781−2793.
(30) Park, K. C.; Levon, K. *Macromolecules* **1997**, *30*, 3175−3183.
(31) Rabolt, J. F.; Hofer, D.; Miller, R. D.; Fickes, G. N. *Macromolecules* **1986**, *19*, 611−616.

developed for bulk polymeric materials. The generic Williams−Landel−Ferry (WLF) equation is unable to describe the variation of the associated "shift" factors with temperature. However, an Arrhenius-type model is able to describe the observed behavior, with an activation enthalpy similar to that associated with rotation around a single carbon−carbon bond. Together with thermodynamic data for interconversion of the two structural forms, this points to secondary motions of hexyl side-chains as dominating film dynamics.

Acknowledgment. We thank the EPSRC (GR/N00968), the British Council and the University of Leicester for financial support. We also thank Dr. S. J. Martin for helpful discussions.

JA0437508